

# Unraveling the role of vacancies in the potentially promising thermoelectric clathrates $\text{Ba}_8\text{Zn}_x\text{Ge}_{46-x-y}\square_y$

Amrita Bhattacharya<sup>1,\*</sup> and Saswata Bhattacharya<sup>2,†</sup><sup>1</sup>*Fritz Haber Institute of the Max Planck Society, Faradayweg 4-6, 14195 Berlin, Germany*<sup>2</sup>*Indian Institute of Technology Delhi, Hauz Khas, New Delhi 110016, India*

(Received 6 May 2016; revised manuscript received 28 August 2016; published 16 September 2016)

Using density-functional theory we compute the formation energies of vacancies  $\square$  in the framework of type I  $\text{Ba}_8\text{Zn}_x\text{Ge}_{46-x-y}\square_y$  clathrates as a function of Zn substitutions. While resolving the contradiction on the experimental reports on the relation between the concentration of Zn,  $x$ , and the number of framework vacancies,  $y$ , our study confirms the observations that vacancies are destabilized with the increase in  $x$ : Up to three vacancies per formula unit can be stabilized for  $0 \leq x < 6$ , while they are unstable for  $x \geq 6$ . This behavior arises from the lower formation energy of (charged) Zn substitution in the Ge framework as compared to a (charged) vacancy creation. Finally our study reveals the stability of a high-temperature  $T$  phase  $\text{Ba}_8\text{Zn}_6\text{Ge}_{40}$  that has high electronic carrier concentration, whereby the carriers also show high- $T$ -induced variation effective for its thermoelectric application.

DOI: [10.1103/PhysRevB.94.094305](https://doi.org/10.1103/PhysRevB.94.094305)

Type I inorganic clathrates are low-density cagelike structures of hosts  $H$  from group 14 that encapsulate guests  $G$  generally from groups IA and IIA (cf. Fig. 1). They offer ample opportunities to tune the electronic and vibrational transport coefficients. In most cases, experimental [1–3] and theoretical [4,5] efforts have mainly aimed at (a) understanding and controlling the vibrational thermal conductivity induced by filling with different guests [1] and (b) tuning the electronic transport coefficients by substitutional doping in the host framework [6]. In the latter case, the compounds  $G_8S_xH_{46-x}$  with their framework substituted by group VIII, IB, IIB, or IIIA elements  $S$  (cf. Fig. 1) have attracted considerable interest as potential candidates for thermoelectric power generation [6–8]. In fact, a figure of merit ( $zT$ ) of  $\sim 1.4$  has been achieved in  $\text{Ba}_8\text{Ga}_{16}\text{Ge}_{30}$  [9–11], which is to date reported to be the highest among intermetallic clathrates [12]. However, the presence of guests or framework substitution also leads to unexpected structural changes, such as the formation of vacancies  $\square$  in the host framework of the clathrates [13–21]. Simple concepts such as the Zintl’s rule have been useful to some extent to rationalize these effects [13,14]; however, the exact understanding of the mechanisms and their impact on the electronic and transport properties are largely unknown. Recent theoretical study in K/Ba guests-filled Si/Ge clathrates revealed that the occurrence of vacancies in these binary clathrate phases is largely driven by the properties of the host framework irrespective of the metal guests [22].

Prior to any framework substitution, a Ba-filled Ge clathrate is found to have three framework vacancies per formula unit (with chemical formula  $\text{Ba}_8\text{Ge}_{43}\square_3$ ). The number of framework vacancies is reported to vary with the type and concentration of the substituted host [19,21,23,24]. The  $\text{Ba}_8\text{Zn}_x\text{Ge}_{46-x-y}\square_y$  series with the framework partially substituted by Zn was first synthesized by Kuhl *et al.* [19]. Based on their x-ray diffraction study, they reported that the number

of framework vacancies ( $y$ ) decreases with the increase in Zn substitution ( $x$ ) following  $y = 4 - x/2$ . Later Alleno *et al.* from their electron probe microanalysis arrived at a different relation:  $y = 3.3 - 0.54x$  for  $0 \leq x < 6$  and  $y = 0$  for  $6 \leq x \leq 8$  [24]. Apart from the exact relation between  $x$  and  $y$ , a complete theoretical understanding of this variation and its impact on the electronic structure of the compositions are hitherto unknown. The composition  $\text{Ba}_8\text{Zn}_8\text{Ge}_{38}$  of the series has shown thermoelectric potential with  $zT$  slightly lower than  $\text{Ba}_8\text{Ga}_{16}\text{Ge}_{30}$  at 300 K [24]. Naturally the electronic, vibrational, and transport properties of several members of the  $\text{Ba}_8\text{Zn}_x\text{Ge}_{46-x-y}\square_y$  series have been studied [25,26]. However, without prior knowledge of the structure and stability of the whole series, the studies focused on the electronic and vibrational transport properties of any particular member of the series is not advantageous.

Identifying the actual number of vacancies at a given concentration of Zn, understanding the mechanisms that favor the vacancy formation at one concentration of Zn but hinder it at the other, and revealing its interplay with the electronic structure are thus important steps towards an atomistic understanding of this material class and, hence, may improve their thermoelectric application.

We address these open questions with first-principles calculations using density-functional theory (DFT) [27,28]. All calculations are performed with FHI-aims [29], an all-electron, full potential electronic structure code that uses numeric, atom-centered basis sets. For all compositions the atomic as well as the geometric relaxations were performed using the Broyden-Fletcher-Goldfarb-Shanno (BFGS) algorithm [30,31].

To ensure that our findings are not an artifact of the chosen treatment for the exchange and correlation (XC), we have first benchmarked the XC functionals, i.e., the local-density approximation (LDA [32]) and several variants of the generalized gradient approximation [PBE [33], PBEsol [34], and RPBE [35]] against the higher-level, computationally more involved hybrid functional HSE06 [36], which incorporates a fraction of exact exchange. We find that for the most vital processes involved, i.e., substitution of a Zn atom in the framework or the formation of the framework vacancy, the PBEsol functional

\*Present address: National Physical Laboratories, New Delhi-110012, India; amrita@fhi-berlin.mpg.de

†saswata@physics.iitd.ac.in

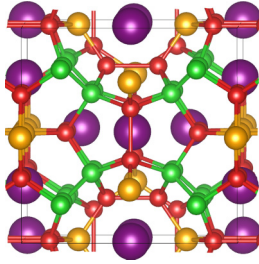


FIG. 1. Crystal structure of type I  $G_8H_{46}$  clathrates (space group  $pm\bar{3}n$ ). Eight guest atoms are accommodated on the  $2a$  and  $6d$  sites (violet). The vacancies and Zn/Ge atoms occupy the Wyckoff sites:  $6c$  (yellow),  $16i$  (green), and  $24k$  (red).

(which is a modified PBE functional for solids) most closely reproduces the results from the HSE06 functional. Therefore, the results presented below are performed using PBEsol functional. A more detailed discussion on the validation of the choice of XC functionals is provided in the Supplemental Material [37].

The formation energies are calculated using the total energies of the diamond Ge ( $\text{Ge}_2^{\text{Dia}}$ ), hexagonal-close-packed Zn ( $\text{Zn}_2^{\text{hcp}}$ ), and the thermodynamically neighboring phase  $\text{BaGe}_2$  [38] as the references for the atomic chemical potentials

$$E_f(x, y) = E(\text{Ba}_8\text{Zn}_x\text{Ge}_{46-x-y}\square_y) - \frac{x}{2}E(\text{Zn}_2^{\text{hcp}}) - \frac{30-x-y}{2}E(\text{Ge}_2^{\text{Dia}}) - 8E(\text{BaGe}_2). \quad (1)$$

In the equation, the coefficients of the second, third, and fourth terms on the right-hand side stoichiometrically balance the number of Zn, Ge, and Ba atoms, respectively, in  $\text{Ba}_8\text{Zn}_x\text{Ge}_{46-x-y}\square_y$ .

The effect of temperature  $T$  on the  $E_f$  is incorporated by adding the contributions stemming from the vibrational free energies  $F_{\text{vib}}$  [39] and the configurational entropy  $S^{\text{Conf}}$  [40] arising from arrangements of defects in the lattice [41]:

$$E_f(x, y, T) = E_f(x, y) + F_{\text{vib}}(T) - TS^{\text{Conf}}. \quad (2)$$

The second term,  $F_{\text{vib}}(T)$ , is the free-energy contribution of the individual compositions appearing in Eq. (1):

$$F_{\text{vib}}(T) = F(\text{Ba}_8\text{Zn}_x\text{Ge}_{46-x-y}\square_y) - \frac{x}{2}F(\text{Zn}_2^{\text{hcp}}) - \frac{30-x-y}{2}F(\text{Ge}_2^{\text{Dia}}) - 8F(\text{BaGe}_2). \quad (3)$$

Finally, the effect of external pressure  $P$  is included in the  $E_f$  by subjecting each of the unit cells in Eq. (1) to external hydrostatic pressure by including the stress tensor directly into the Hamiltonian [42].

To determine the stable vacancy compositions as a function of Zn substitutions in the Ge framework, we first identified the energetically most favorable geometric configurations for the compositions  $\text{Ba}_8\text{Zn}_x\text{Ge}_{46-x-y}\square_y$  with concentration of Zn  $x \in [0, 10]$ . For this purpose, we adopted an iterative strategy: Starting with the completely filled clathrate  $\text{Ba}_8\text{Ge}_{46}$ , we first identified the most favorable sites for the Zn substitution by scanning over all possible framework positions. For subsequent Zn substitution, we retained the previous composi-

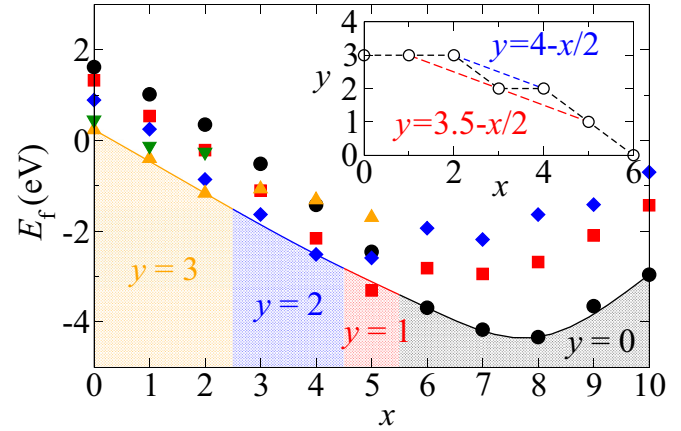


FIG. 2. The formation energy  $E_f$  of  $\text{Ba}_8\text{Zn}_x\text{Ge}_{46-x-y}\square_y$  clathrates as a function of the number of Zn atoms,  $x$ , per formula unit. The solid symbols  $\circ$ ,  $\square$ ,  $\diamond$ ,  $\triangle$ , and  $\nabla$  correspond to the compositions with numbers of vacancies  $y = 0, 1, 2, 3$ , and  $4$ , respectively. The inset shows the number of vacancies,  $y$ , in the most favorable compositions as a function of  $x$  for  $0 \leq x \leq 6$ .

tion and scanned over the rest of the available framework sites. Analogously, with the identified composition  $\text{Ba}_8\text{Zn}_x\text{Ge}_{46-x}$ , we have stepwise taken out the Ge host atoms by scanning over all the framework sites. For subsequent vacancy, we retained the vacancy at the already-identified position and scanned over the rest of the available framework sites. Eventually, we calculated the formation energies of the phases using Eq. (1).

For the substitutions of the first six Zn atoms, the occupation of  $6c$  positions are found to be energetically more favorable than that of the  $16i$  and  $24k$  positions. Following the complete occupation of the  $6c$ , the substitutions at the  $16i$  and/or  $24k$  positions take place. The vacancies also show a preference of the  $6c$  positions as long as the Ge-occupied  $6c$  positions are available after the Zn substitutions. As shown in Fig. 2, the number of vacancies,  $y$ , in the most stable composition decreases with increase in  $x$ . In the Zn-deficient condition, i.e., at  $x = 0$ , the most stable composition ( $\text{Ba}_8\text{Ge}_{43}\square_3$ ) is found to have three vacancies in the framework as observed experimentally [17,43]. Our results show that vacancies are present in compositions for  $0 < x < 6$ , whereby  $y$  varies differently as  $y = 4 - x/2$  and  $y = 3.5 - x/2$  for the even and odd concentrations of  $x$ , respectively (cf. inset of Fig. 2). Thus, our results show that the relation drawn by Kuhl *et al.* is exactly valid for the compositions with  $x = 2, 4$  [19], while the relation established by Alleno *et al.* is roughly followed by the compositions with  $x = 1, 3, 5$  [24]. Framework vacancies are found to be unstable for  $x \geq 6$ . The low energy compositions at different values of  $x$  form a convex hull, whereby  $\text{Ba}_8\text{Zn}_8\text{Ge}_{38}$  comprises the energy minimum as found experimentally [19,24].

To investigate whether the identified most favorable clathrates at 0 K are also the most stable ones at finite temperature  $T$ , we have computed their thermodynamic stability using Eq. (2). We have first calculated the thermodynamic stabilities of vacancies in  $\text{Ba}_8\text{Zn}_x\text{Ge}_{46-x-y}\square_y$  for a given  $x \in [0, 8]$ . Four such cases are shown in Fig. 3(a). We find that the most stable compositions at 0 K also retain their stabilities at the  $T$  range of 0–1600 K for all  $x$ . Subsequently, we have

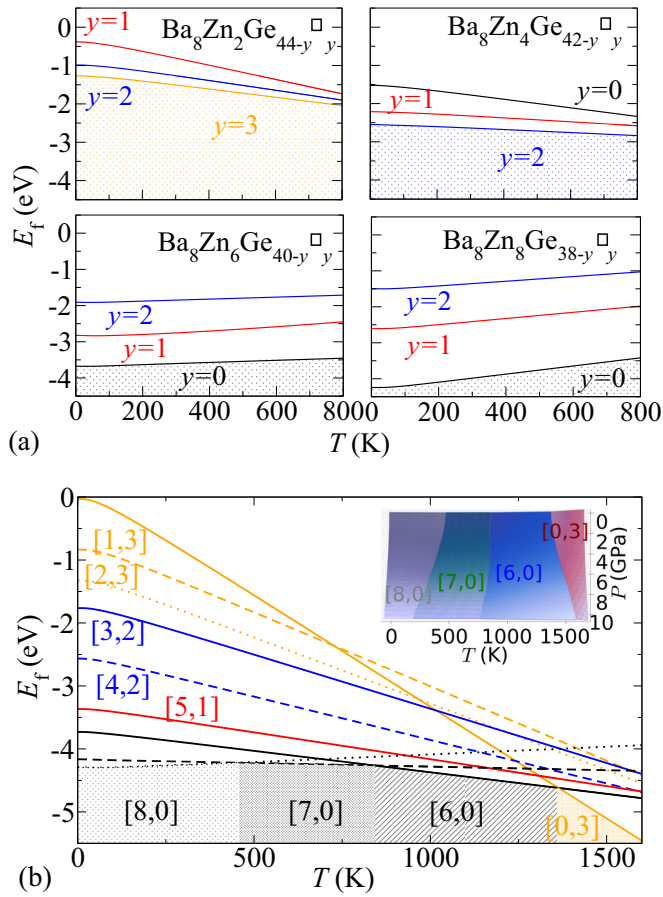


FIG. 3. (a) Formation energy  $E_f$  of  $\text{Ba}_8\text{Zn}_x\text{Ge}_{46-x-y}\square_y$  plotted as a function of temperature  $T$  for vacancies  $\square_y$  at a given concentration of Zn substitution  $x$  in the framework. (b) Formation energy comparison of the most stable compositions for  $x \in [0, 0.8]$  as a function of temperature  $T$ . The different compositions are labeled  $[x, y]$  according to the concentration of Zn,  $x$ , and number of vacancies,  $y$ , per formula unit. The inset shows the aerial perspective of the  $E_f$  of the most stable phases plotted as a function of  $T$  and pressure  $P$ .

compared the thermodynamic stabilities for each of the most stable compositions for  $x \in [0, 0.8]$  [cf. Fig. 3(b)].  $\text{Ba}_8\text{Zn}_8\text{Ge}_{38}$  is found to be the most stable composition in the  $T$  range 0–450 K. Interestingly, we find that concentration of Zn in the most stable composition decreases with increasing  $T$ . At  $T$  range 480–830 K,  $\text{Ba}_8\text{Zn}_7\text{Ge}_{39}$  is found to be the most stable phase.  $\text{Ba}_8\text{Zn}_6\text{Ge}_{40}$  is found to be the most favorable phase at higher  $T$  (850–1350 K). Beyond this, the energetically adverse composition  $\text{Ba}_8\text{Zn}_4\text{Ge}_{42}\square_3$  is found to be thermodynamically the most favorable composition. The thermodynamic stabilities of the most favorable compositions are also retained at finite  $P$  as shown in the inset of Fig. 3(b). At higher pressure  $P$  (10 GPa), the phase  $\text{Ba}_8\text{Zn}_6\text{Ge}_{40}$  is found to be stable over broad  $T$  range (750–1500 K).

Microscopically the impact of the substituted Zn atom and/or the framework vacancy on the stability of the compositions can be analyzed by plotting the individual defect formation energies [ $E_f(\square^q)$  and  $E_f(\text{Zn}^q)$ ] as a function of the electron chemical potential  $\mu_e$  [cf. Fig. 4(a)]. The single charged

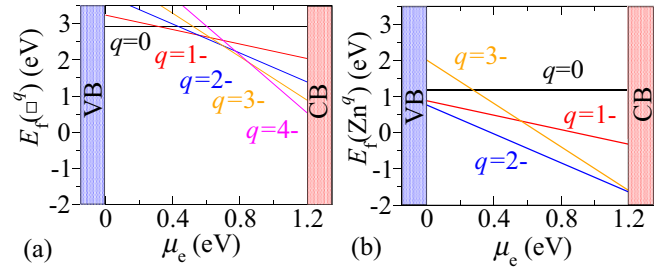


FIG. 4. The defect formation energies in the empty clathrate framework as a function of the electron chemical potential  $\mu_e$  for charge states  $q$ : (a)  $E_f(\square^q)$  for a single vacancy  $\square$  and (b)  $E_f(\text{Zn}^q)$  for a single Zn atom substitution.

vacancy formation energy in the empty clathrate framework is calculated using [44]

$$E_f(\square^q) = E(\text{Ge}_{45}\square_1^q) - E(\text{Ge}_{46}) + \frac{E(\text{Ge}_2^{\text{Dia}})}{2} + q(\mu_e + \text{VBM} + \Delta V), \quad (4)$$

in which  $E(\text{Ge}_{45}\square_1^q)$  denotes the total energy of the host framework with one vacancy at charge  $q$ ,  $E(\text{Ge}_{46})$  is the one of the pristine clathrate, and  $E(\text{Ge}_2^{\text{Dia}})$  is the one of the diamond phase. Furthermore,  $\mu_e$  is the chemical potential relative to the valence-band maximum (VBM) of the pristine clathrate, and  $\Delta V$  accounts for the core level alignment between  $E(\text{Ge}_{45}\square_1^q)$  and  $E(\text{Ge}_{46})$ .

Similarly, for a single Zn atom substitution in the framework, the charged Zn formation energy can be calculated using

$$E_f(\text{Zn}^q) = E(\text{Zn}^q\text{Ge}_{45}) - E(\text{Ge}_{46}) + \frac{E(\text{Ge}_2^{\text{Dia}})}{2} - \frac{E(\text{Zn}_2^{\text{hcp}})}{2} + q(\mu_e + \text{VBM} + \Delta V'), \quad (5)$$

in which  $E(\text{Zn}^q\text{Ge}_{45})$  denotes the total energy of the host framework with one Ge atom substituted by one Zn atom. The atomic chemical potential for the substituted Zn atom is its bulk hcp phase  $\text{Zn}_2^{\text{hcp}}$  while the atomic chemical potential for the substituted Ge atom is the same as before ( $\text{Ge}_2^{\text{Dia}}$ ).  $\Delta V'$  accounts for the core level alignment between  $E(\text{Zn}^q\text{Ge}_{45})$  and  $E(\text{Ge}_{46})$ .

The vacancy in the framework shows charge states of  $q = 0, 1-, \dots, 4-$  for  $\mu_e$  values in the band gap [cf. Fig. 4(a)]. The neutral vacancy formation energy  $E_f(\square^0) |_{\mu_e=\text{VBM}}$  is significantly positive,  $\sim 2.9$  eV, which, however, gets reduced when the electronic vacancy states are occupied. The completely charged vacancy formation energy  $E_f(\square^{4-}) |_{\mu_e=\text{CBM}}$  is found to be  $\sim 0.38$  eV [cf. Fig. 4(a)]. In contrast, the substituted Zn atom has a charge state of  $q = 2-$  for all values of  $\mu_e$  varying in the band gap. In the  $p$ -type host, when  $\mu_e$  is close to VBM,  $E_f(\text{Zn}^{2-}) |_{\mu_e=\text{VBM}}$  is also significantly positive 0.76 eV. However, in an extremely  $n$ -type host,  $E_f(\text{Zn}^{2-}) |_{\mu_e=\text{CBM}}$  is lowered to  $\sim -1.6$  eV [cf. Fig. 4(b)]. Therefore, Zn substitution is found to be energetically more favorable than the formation of framework vacancy by  $\sim 2.0$  eV for all values of  $\mu_e$ . Moreover, two substituted Zn atoms can exactly balance one completely charged vacancy electronically. Naturally,

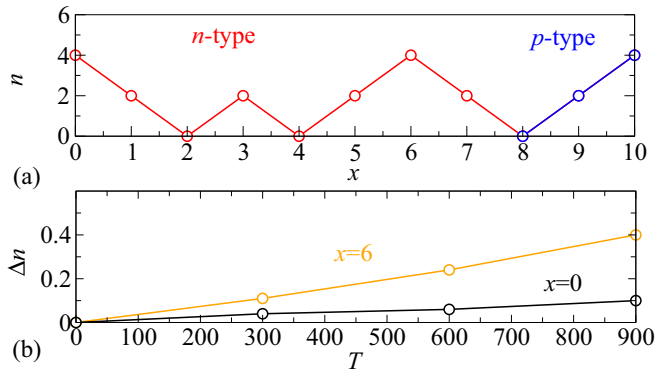


FIG. 5. (a) Computed number of carriers in the conduction band in  $\text{Ba}_8\text{Zn}_x\text{Ge}_{46-x-y}\square_y$  as a function of substituted Zn atoms  $x$  per formula unit. (b) Change in the charge carriers  $n$  as a function of  $T$  for compositions  $\text{Ba}_8\text{Ge}_{43}\square_3$  ( $x = 0$ ) and  $\text{Ba}_8\text{Zn}_6\text{Ge}_{40}$  ( $x = 6$ ).

vacancies occur only in Zn-deficient conditions, and with the increase in Zn concentration the number of vacancies in the framework decreases.

Figure 5 summarizes the electronic structures of the lowest-energy compositions as a function of  $x$ . The composition  $\text{Ba}_8\text{Ge}_{43}\square_3$  shows a metallic state with four electrons in the conduction band. Since only 12 out of the 16 electrons donated by the eight Ba guests are balanced by the three framework vacancies, the surplus four electrons occupy the states in the conduction band. The first two Zn substitutions balance the surplus four electrons, leading to a semiconducting state in  $\text{Ba}_8\text{Zn}_2\text{Ge}_{41}\square_3$  with a band gap of 0.01 (PBEsol)/0.1 (HSE06) eV. Beyond this, Zn substitutions only take place at the expense of framework vacancies, which provides the necessary electrons for its charging. Thus, the composition  $\text{Ba}_8\text{Zn}_4\text{Ge}_{40}\square_2$  is also found to have a semiconducting state, with a band gap of 0.03 (PBEsol)/0.21 (HSE06) eV, whereby the two vacancies and four Zn atoms exactly balance the 16 electrons donated by Ba guests. The compositions at  $x = 1, 3, 5$  are found to be metallic, since uncompensated electrons remain following the relation  $y = 3.5 - x/2$ . At  $x = 8$ , the electrons donated by the Ba guests are completely balanced by the eight Zn atoms. Thus,  $\text{Ba}_8\text{Zn}_8\text{Ge}_{38}$  is a semiconductor with a band gap of 0.15 (PBEsol)/0.54 (HSE06) eV. Subsequent substitutions of Zn are found to be energetically less favorable, since surplus electrons are not available for their charging. For Zn substitutions beyond  $x = 8$ , the holes act as carriers, whereby the further substituted Zn atom undergoes a  $p$ -type doping. All Zn-substituted compositions show a tendency towards complete balance of electronic charge [45], except  $\text{Ba}_8\text{Zn}_6\text{Ge}_{40}$ , which does not feature the additional framework vacancy even though four surplus electrons are available. The reason is traced from the stiffness analysis of the phases discussed below. Therefore, on an electronic level, all compositions are found to obey Zintl's rule.

Finally, from the perspective of thermoelectric application of these compositions it is very crucial to study the behavior of the electronic charge carriers as a function of the temperature  $T$ . For this purpose, we have calculated the  $T$ -induced variations in the charge-carrier concentrations  $n$  [46] for the thermodynamically stable most metallic compositions,

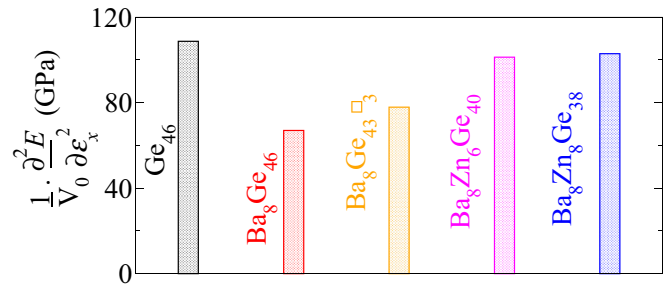


FIG. 6. The second-order strain derivatives of the total energies  $E$  as a function of uniaxial strain  $\epsilon_x$  for crystals with equilibrium volume  $V_0$ .

viz., the vacancy-rich  $\text{Ba}_8\text{Ge}_{43}\square_3$  ( $x = 0$ ) and the Zn-rich  $\text{Ba}_8\text{Zn}_6\text{Ge}_{40}$  ( $x = 6$ ) as shown in Fig. 5(b).  $\text{Ba}_8\text{Ge}_{43}\square_3$  shows a bad metallic behavior, whereby  $n$  is found to be weakly dependent on  $T$ . However, the slope  $\frac{\Delta n}{\Delta T}$  is found to be about four times higher in  $\text{Ba}_8\text{Zn}_6\text{Ge}_{40}$ , suggesting a more metallic trait. The high electron count and the higher  $T$  dependence of the charge carriers in  $\text{Ba}_8\text{Zn}_6\text{Ge}_{40}$  are preliminary positive signatures for its thermoelectric application.

Figure 6 shows the comparison of the second-order strain derivative of the total energy  $E$  per unit volume  $\frac{1}{V_0} \frac{\partial^2 E}{\partial \epsilon_x^2}$  of the isotropic ( $\text{Ge}_{46}$  and  $\text{Ba}_8\text{Zn}_6\text{Ge}_{40}$ ) and nonisotropic ( $\text{Ba}_8\text{Ge}_{46}$ ,  $\text{Ba}_8\text{Ge}_{43}\square_3$ , and  $\text{Ba}_8\text{Zn}_8\text{Ge}_{38}$ ) phases [47]. In the case of the isotropic crystal, this is equivalent to the Young modulus ( $Y$ ) of the crystal, whereas in general it is an estimation of the rigidity or stiffness. The empty clathrate cage  $\text{Ge}_{46}$  is found to be stiffest of all the analyzed phases ( $Y = 108$  GPa), whereby filling of the cage with Ba guests leads to softening of the crystal bonds. Consequently,  $\text{Ba}_8\text{Ge}_{46}$  has a drastically low stiffness of  $Y = 67$  GPa ( $\sim 40\%$  lower than that of  $\text{Ge}_{46}$ ). This softening favors the formation of framework vacancies, by means of which the surplus electrons donated by the guests are balanced. Thus, the intrinsic strength of the crystal is increased by  $\sim 17\%$ , leading to a stiffness of 78 GPa. The balance of electronic charge also occurs upon substitution of the Zn atoms in the framework. However, in this case, the intrinsic strength of the crystal is found to be hardly affected (close to that of  $\text{Ge}_{46}$ ), since the overall cage structure is retained upon Zn substitution. The stiffness of the  $\text{Ba}_8\text{Zn}_6\text{Ge}_{40}$  and  $\text{Ba}_8\text{Zn}_8\text{Ge}_{38}$  phases are found to be very close in spite of the complete balance of electrons occurring only in the latter case. This is due to the crystal symmetry that is retained in  $\text{Ba}_8\text{Zn}_6\text{Ge}_{40}$ , which opposes the creation of the additional framework vacancy required to balance the surplus electronic charge.

In summary, we have performed first-principles calculations to investigate the stoichiometries, thermodynamic stabilities, and electronic structures of the  $\text{Ba}_8\text{Zn}_x\text{Ge}_{46-x-y}\square_y$  series. Our study confirms several experimental observations. Formation of up to three vacancies is energetically favorable for  $0 \leq x < 6$ , while vacancies are not favorable for  $x \geq 6$ . This resolves the conflicts on the exact relation between  $y$  and  $x$  observed experimentally. We find  $y$  varies differently as  $y = 4 - x/2$  (in agreement with Kuhl *et al.* [19]) and  $y = 3.5 - x/2$  (roughly in agreement with Alleno *et al.* [24]) for the even and odd concentrations of  $x$ , respectively. The formation of the neutral vacancy or the substitution of a

neutral Zn atom is energetically unfavorable, but high energetic gain occurs whenever the electronic vacancy states or the electronic valence orbitals of Zn are occupied. Each  $\square$  can accommodate up to four electrons, while each substituted Zn atom accommodates two electrons. Thus, two Zn substitutions can exactly electronically balance the completely charged vacancy and the process is found to be energetically favorable by more than  $\sim 2$  eV per Zn substitution. Therefore, vacancies only occur in Zn-deficient conditions. All compositions of the  $\text{Ba}_8\text{Zn}_x\text{Ge}_{46-x-y}\square_y$  series satisfy the Zintl condition. All Zn-substituted compositions show a tendency towards complete balance of the surplus electronic charge except  $\text{Ba}_8\text{Zn}_6\text{Ge}_{40}$ , which does not feature the additional vacancy in

spite of the availability of the four surplus electrons. This is due to its isotropic symmetric structure that generates exceptional intrinsic strength which impedes the additional vacancy formation. The charge carriers in  $\text{Ba}_8\text{Zn}_6\text{Ge}_{40}$  show high temperature dependence as compared to those in bad metallic  $\text{Ba}_8\text{Ge}_{43}\square_3$ . Thus,  $\text{Ba}_8\text{Zn}_6\text{Ge}_{40}$  shows positive behavior crucial for its thermoelectric application.

A.B. acknowledges Christian Carbogno and Matthias Scheffler for introducing her to this field. The thermoelectrics group of Yuri Grin at MPI-CPfS, Dresden, is acknowledged for the ongoing collaboration. We acknowledge the high-performance computing facility of IIT Delhi.

- 
- [1] J. L. Cohn, G. S. Nolas, V. Fessatidis, T. H. Metcalf, and G. A. Slack, *Phys. Rev. Lett.* **82**, 779 (1999).
- [2] J. S. Tse, K. Uehara, R. Rousseau, A. Ker, C. I. Ratcliffe, M. A. White, and G. MacKay, *Phys. Rev. Lett.* **85**, 114 (2000).
- [3] G. S. Nolas, G. A. Slack, and S. B. Schujman, *Semiconductors and Semimetals* (Academic Press, Boca Raton, FL, 2001), Vol. 29, Chap. 6.
- [4] J. Dong, O. F. Sankey, and C. W. Myles, *Phys. Rev. Lett.* **86**, 2361 (2001).
- [5] Y. He and G. Galli, *Nano Lett.* **14**, 2920 (2014).
- [6] M. Christensen, S. Johnsen, and B. B. Iversen, *Dalton Trans.* **39**, 978 (2010).
- [7] A. D. McNaught and A. Wilkinson, *IUPAC: Compendium of Chemical Terminology* (Blackwell Scientific Publications, Oxford, 1997).
- [8] T. Takabatake, K. Suekuni, T. Nakayama, and E. Kaneshita, *Rev. Mod. Phys.* **86**, 669 (2014).
- [9] A. Sarmat, G. Svensson, A. E. C. Palmqvist, C. Stiewe, E. Mueller, D. Platzek, S. G. K. Williams, D. M. Rowe, J. D. Bryan, and G. D. Stucky, *J. Appl. Phys.* **99**, 023708 (2006).
- [10] M. Christensen, N. Lock, J. Overgaard, and B. B. Iversen, *J. Am. Chem. Soc.* **128**, 15657 (2006).
- [11] E. S. Toberer, M. Christensen, B. B. Iversen, and G. J. Snyder, *Phys. Rev. B* **77**, 075203 (2008).
- [12] H. Kleinke, *Chem. Mater.* **22**, 604 (2010).
- [13] H. G. von Schnering, *Nova Acta Leopold.* **59**, 165 (1985).
- [14] H. G. von Schnering, *Bol. Soc. Chil. Quim.* **33**, 41 (1988).
- [15] H. G. von Schnering, J. Llanos, K. Peters, M. Baitinger, Y. Grin, and R. Nesper, *Z. Kristallogr. New Cryst. Struct.* **226**, 9 (2011).
- [16] F. Dubois and T. F. Fassler, *J. Am. Chem. Soc.* **127**, 3264 (2005).
- [17] U. Aydemir, C. Candolfi, H. Borrmann, M. Baitinger, A. Ormeci, W. Carrillo-Cabrera, C. Chubilleau, B. Lenoir, A. Dauscher, N. Oeschler, F. Steglich, and Y. Grin, *Dalton Trans.* **39**, 1078 (2010).
- [18] J.-T. Zhao and J. D. Corbett, *Inorg. Chem.* **33**, 5721 (1994).
- [19] B. Kuhl, A. Czybulka, and H.-U. Schuster, *Anorg. Allg. Chem.* **621**, 1 (1995).
- [20] U. Aydemir, C. Candolfi, A. Ormeci, H. Borrmann, U. Burkhardt, Y. Oztan, N. Oeschler, M. Baitinger, F. Steglich, and Y. Grin, *Inorg. Chem.* **51**, 4730 (2012).
- [21] U. Aydemir, C. Candolfi, A. Ormeci, M. Baitinger, N. Oeschler, F. Steglich, and Y. Grin, *J. Phys.: Condens. Matter* **26**, 485801 (2014).
- [22] A. Bhattacharya, C. Carbogno, B. Böhme, M. Baitinger, Y. Grin, and M. Scheffler, *Phys. Rev. Lett.* (unpublished).
- [23] S. Y. Rodriguez, L. Saribaev, and J. H. Ross, *Phys. Rev. B* **82**, 064111 (2010).
- [24] E. Alleno, G. Maillet, O. Rouleau, E. Leroy, C. Godart, W. Carrillo-Cabrera, P. Simon, and Y. Grin, *Chem. Mater.* **21**, 1485 (2009).
- [25] N. Melnychenko-Koblyuk, A. Grytsiv, L. Fornasari, H. Kaldarar, H. Michor, F. Röhrbacher, M. Koza, E. Royanian, E. Bauer, P. Rogl, M. Rotter, H. Schmid, F. Marabelli, A. Devishvili, M. Doerr, and G. Giester, *J. Phys.: Condens. Matter* **19**, 216223 (2007).
- [26] M. Christensen and B. B. Iversen, *J. Phys.: Condens. Matter* **20**, 104244 (2008).
- [27] P. Hohenberg and W. Kohn, *Phys. Rev.* **136**, B864 (1964).
- [28] W. Kohn and L. J. Sham, *Phys. Rev.* **140**, A1133 (1965).
- [29] V. Blum, R. Gehrke, F. Hanke, P. Havu, V. Havu, X. Ren, K. Reuter, and M. Scheffler, *Comput. Phys. Commun.* **180**, 2175 (2009).
- [30] D. Frenkel and B. Smit, *Understanding Molecular Simulation* (Academic Press, San Francisco, 2002).
- [31] The generalized forces are converged to smaller than  $10^{-3}$  eV/Å. Converged reciprocal space grids ( $8 \times 8 \times 8$ ) per unit cell with converged “tight” basis sets are used. The chosen numerical settings yield a convergence for energy differences of  $< 10^{-3}$  eV/atom.
- [32] J. P. Perdew and Y. Wang, *Phys. Rev. B* **45**, 13244 (1992).
- [33] J. P. Perdew, K. Burke, and M. Ernzerhof, *Phys. Rev. Lett.* **77**, 3865 (1996).
- [34] J. P. Perdew, A. Ruzsinszky, G. I. Csonka, O. A. Vydrov, G. E. Scuseria, L. A. Constantin, X. Zhou, and K. Burke, *Phys. Rev. Lett.* **100**, 136406 (2008).
- [35] B. Hammer, L. B. Hansen, and J. K. Nørskov, *Phys. Rev. B* **59**, 7413 (1999).
- [36] A. V. Krukau, O. A. Vydrov, A. F. Izmaylov, and G. E. Scuseria, *J. Chem. Phys.* **125**, 224106 (2006).
- [37] See Supplemental Material at <http://link.aps.org/supplemental/10.1103/PhysRevB.94.094305> for comparison of the neutral and charged formation energies for the vacancy creation and Zn substitution in the empty clathrate framework with various XC functionals and justify the choice of PBEsol functional for performing the calculations.

- [38] W. Carrillo-Cabrera, J. Curda, H. G. von Schnering, S. Paschen, and Y. Grin, *Z. Kristallogr. New Cryst. Struct.* **215**, 207 (2000).
- [39] The  $F_{\text{vib}}$  is calculated with the harmonic approximation using the PHONOPY code for the postprocessing of the harmonic force constants generated by the finite displacement method.
- [40]  $S^{\text{Conf}} = K_B \frac{N_{\text{tot}}!}{N_s!(N_{\text{tot}}-N_s)!}$ , where  $N_{\text{tot}}$  is the total number of sites,  $N_s$  is the number of degenerate sites available for the vacancies or Zn substitution, and  $K_B$  is the Boltzmann constant.
- [41] C. Kittel, *Introduction to Solid State Physics*, 8th ed. (John Wiley and Sons, New York, 2005), Chap. 20.
- [42] F. Knuth, C. Carbogno, V. Atalla, V. Blum, and M. Scheffler, *Comput. Phys. Commun.* **190**, 33 (2015).
- [43] C. Candolfi, U. Aydemir, M. Baitinger, N. Oeschler, F. Steglich, and Y. Grin, *J. Electron. Mater.* **39**, 2039 (2010).
- [44] C. Freysoldt, B. Grabowski, T. Hickel, J. Neugebauer, G. Kresse, A. Janotti, and C. G. Van de Walle, *Rev. Mod. Phys.* **86**, 253 (2014).
- [45] The compositions with  $x = 1, 3, 5$  are found to be metallic. But they do not have surplus four electrons available to support one extra charged vacancy in the framework .
- [46] For each  $T \in 300, 600, 900$  K for the given compositions, 5-ps-long Molecular Dynamics simulations (time step 3 fs) are performed using the NVT-Parrinello thermostat [R. Car and M. Parrinello, *Phys. Rev. Lett.* **55**, 2471 (1985)]. We then take three snapshots of geometries corresponding to 3, 4, and 5 ps for each  $T$  and calculate the number of electrons in the conduction band of the static density of states. Subsequently, we average them for all the snapshots for the given  $T$ .
- [47]  $\text{Ba}_8\text{Zn}_6\text{Ge}_{40}$  has a perfect cubic crystal structure retaining the  $pm\bar{3}n$  symmetry, since the Zn atoms occupy the degenerate  $6c$  sites.  $\text{Ba}_8\text{Ge}_{46}$  has a tetragonal lattice with one of the lattice parameters undergoing axial elongation. Upon spontaneous creation of the three framework vacancies, the cubic lattice structure is restored but the symmetry is not retained.